Journal of Supramolecular Structure 2:593–608 (1974)

PHYSICAL PROPERTIES OF THE LIPID PHASE OF MEMBRANES FROM CULTURED ANIMAL CELLS

Bernadine J. Wisnieski, Yoshie O. Huang, and C. Fred Fox

Department of Bacteriology and the Molecular Biology Institute, University of California, Los Angeles, California 90024

ESR analysis of membranes from cultured animal cells reveals a more complex lipid phase behavior than that displayed by ideal binary lipid systems. When endoplasmic reticulum membranes from LM cells are spin labeled with a nitroxide derivative of decane, 5N10, and scanned by ESR at 1°C-intervals, the partitioning of 5N10 between the hydrocarbon and aqueous portions of the membrane suspension undergoes thermotropic changes at characteristic temperatures of 9°, 16°, 22°, 32°, and 38°C. Lipids extracted from these same membranes, however, exhibit only two characteristic temperatures, 16° and 35°C, and in this respect resemble binary lipid systems. The phase behavior of lipids in animal cell membranes is suggestive of an organized distribution of lipid which is disrupted by extraction. In support of this, mathematical treatment of the partitioning data indicates that four of these characteristic temperatures can define the boundaries (i.e., the t_l and t_h) of two independent phase transitions in endoplasmic reticulum membranes. These results are similar to those of a physical treatment of data from plasma membranes of both mouse and chick cells in which the two monolayers appear to exist as independent physical entities with different physical properties. The most probable phase boundaries for the two monolayers of the endoplasmic reticulum membranes studied here are 16° and 32°C for one monolayer and 22° and 38°C for the other.

INTRODUCTION

Investigations of membrane lipid phase behavior have typically concentrated on model lipid systems and lipid-requiring strains of microbes. Physical studies on Escherichia coli membranes show that they behave like ideal binary lipid systems in that they display a single lateral phase separation process defined by lower and upper characteristic temperatures, t_l and t_h, respectively. These mark the beginning and end of melting of lipids in the membrane bilayer. Correlations between these physical characteristic temperatures and characteristic temperatures for membrane processes have been demonstrated in E. coli (1–8) and Mycoplasma (9). However, no detailed correlative study

of this sort has been made with animal cell membranes; therefore, much of what is known about lipid phase behavior in animal cells is by inference. Changes in membrane lipid state in animal cell membranes are assumed to occur at temperatures where thermotropic transitions are detected in the activity of a membrane-bound enzyme or in the "mobility" (or activity) of a surface receptor. Confirmation of these assumptions requires that the physical characteristic temperatures of animal cell membranes coincide with the physiological ones.

Recent studies by Wisnieski et al. (10) were undertaken to determine the physical state of the plasma membrane of LM cells, a cultured line of mouse fibroblasts. Electron spin resonance (ESR) studies revealed that extracted lipids from these membranes behaved like ideal binary lipid systems in that they displayed only two characteristic temperatures, a t_l and a t_h. Intact membranes, however, displayed four or more characteristic temperatures by ESR and by biochemical assays of amino acid transport and membrane ATPase. The unusual phase behavior of these membranes was shown to be compatible with a membrane model in which the two monolayers of the membrane bilayer of animal cells exist as independent entities with different physical properties.

In this report, we will summarize the physical and physiological evidence for four characteristic temperatures in the plasma membrane of LM cells and present the results of an ESR study of the physical state of LM endoplasmic reticulum membranes.

MATERIALS AND METHODS

Membrane Isolation

Endoplasmic reticulum membranes were isolated from LM cells maintained as monolayer cultures in Eagle's minimal essential medium (MEM) plus 0.5% peptone (11). Membranes were isolated as described by Schimmel et al. (12) with the following modifications: (1) Before homogenization, the cell suspension was incubated in Earle's salt solution for 10 min. This facilitated lysis during homogenization. (2) 20–30 strokes in a Dounce homogenizer were required for cell disruption. (3) The 1.7×10^4 g · min supernatant fraction was then centrifuged at 2×10^6 g · min. The pellet was suspended and the suspended membranes banded to equilibrium in a sucrose gradient exactly as described by Schimmel et al. Ouabain-sensitive ATPase activity in bands I and II (plasma membrane) was eightfold greater than in the particulate homogenate. The purity of endoplasmic reticulum membranes (band IV) from LM cells was similar to that reported by Schimmel et al. for band IV from cultured chick embryo muscle cells based on enzymic assays.

ESR Samples

One 150 μg (as protein) aliquot of LM endoplasmic reticulum membranes (in 1 mM triethanolamine (TEA · HCl, pH 7.4) was prepared for ESR (see ESR Techniques) immediately after isolation. Two additional 150 μg samples were from preparations which had been stored at −20°C for several days. No differences in the physical properties of fresh and frozen samples were detected by ESR.

Total lipids were extracted from 1.2 mg (as protein) of endoplasmic reticulum

membranes by the method of Bligh and Dyer (13). The lipid extract (approximately 1.0 ml) was filtered through Na_2SO_4 and glass wool, dried under a stream of nitrogen, and suspended in 100 μl of chloroform:methanol (2:1). Small aliquots were repeatedly taken from the 100 μl sample, added to a small glass capillary tube, and dried under nitrogen. When the entire sample had been transferred to the capillary tube and dried, 40 μl of 1 mM TEA·HCl containing 10^{-4} M $K_3Fe(CN)_6$ and 3×10^{-4} M spin label (5N10; see below) were added. The tube was suspended in a water bath at 22°C and sonicated for 30 min using an L&R 430G power supply. A 20 μl portion of the sample was then removed and added to another capillary tube containing 20 μl of the spin label-$K_3Fe(CN)_6$-TEA·HCl solution described above. The sample was incubated at 22°C for at least 24 hr before spectra were taken.

ESR Techniques

Details of the spin labeling method and instrumentation were similar to those published for LM plasma membrane samples and viral lipids (10). Briefly, 100–150 μl aliquots of endoplasmic reticulum suspension containing 150 μg of protein were combined with 4 μl of 10^{-2} M $K_3Fe(CN)_6$ and equilibrated at 22°C for 30 min. Next, 1 μl of 10^{-2} M 5N10 (in ethanol), a nitroxide derivative of decane (2) donated by Dr. A. D. Keith of Pennsylvania State University, was added and the sample equilibrated at 22°C for 30 min. The entire sample was then placed in a capillary tube which had been sealed at one end, and the capillary tube was centrifuged in a Sorvall HB4 swinging bucket rotor for 1 hr at 16,300 × g. Supernatant fluid was removed from the capillary until a 1:1 ratio of supernatant fluid to pellet volume was attained. The tube was sealed and incubated at 0°C for at least 1 hr before taking the first spectrum. ESR spectra were obtained on a Varian 4500-10A spectrometer operating at X-band and equipped with a Varian variable temperature accessory and an X-Y recorder. A copper-constantan thermocouple was inserted into the cavity with the sample capillary and temperatures were monitored before and after each scan on a Leeds and Northrup millivolt potentiometer. The temperatures were estimated to be precise to at least ±0.1°C. Each sample was incubated for 10 min at the indicated temperature and each spectrum was a 5 min scan over a 100 gauss range. Spectra were taken in ascending order from approximately 3° to 43°C.

RESULTS

A typical first derivative ESR spectrum obtained from a biological membrane preparation spin labeled with the nitroxide 5N10 is shown in Fig. 1. The splitting of the ESR high field line indicates that the spin label is partitioning between hydrocarbon and polar environments of the membrane suspension. The amount of spin label in each environment can be calculated from the amplitudes of the hydrocarbon (h_H) and polar (h_P) components of the high field line. The method of measuring h_H and h_P shown in Fig. 1 is similar to that of Shimshick and McConnell (14).

Detection of phase transition boundaries is based on the observation by Hubbell and McConnell (15) that spin labels such as TEMPO are far more soluble in a fluid (F) hydrocarbon phase than in a solid (S) one. In their elegant studies on thermotropic phase

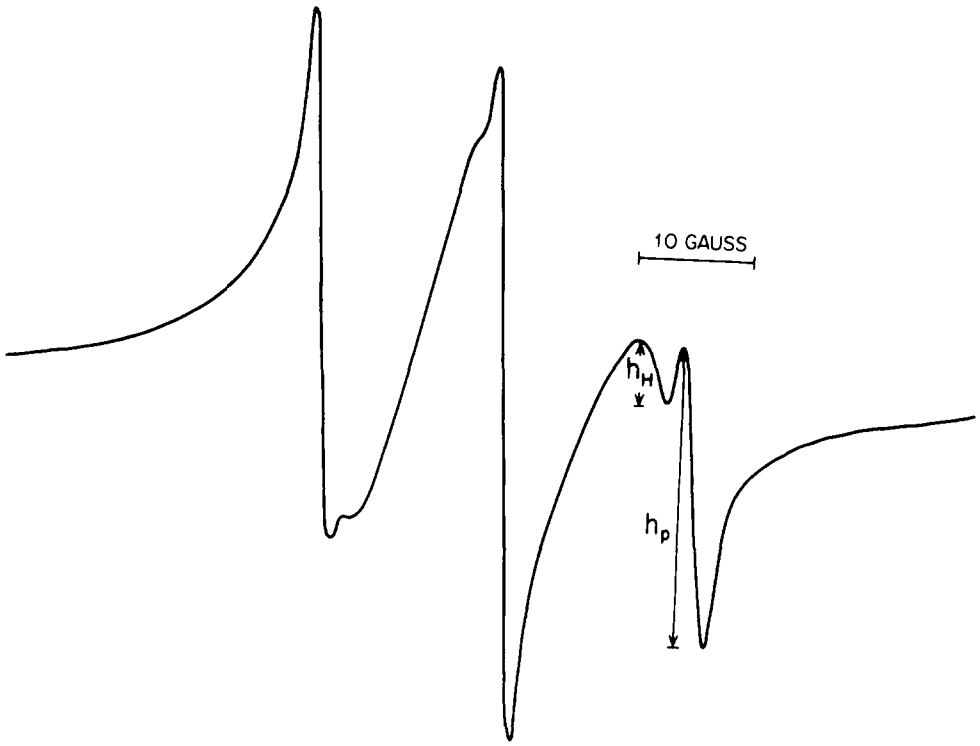

Fig. 1. ESR spectrum at 25°C from an aqueous suspension of endoplasmic reticulum membranes labeled with 5N10. Membranes were derived from LM cells (see Materials and Methods). Heights h_H and h_P define the distribution of spin label in the hydrocarbon and aqueous components of the sample.

transition properties of aqueous binary phospholipid dispersions, Shimshick and McConnell (14) utilized this hydrocarbon solubility property of a spin label probe to detect the upper and lower boundaries of the lipid phase transition. When an aqueous dispersion of phospholipids or membranes is heated over a temperature range where all lipids are in the S state, a plot of the logarithm of the spectral parameter $f = [h_H/(h_H + h_P)]$ has a defined slope as a function of the reciprocal of the absolute temperature. The lower and upper phase transition boundaries are the points where the fluid hydrocarbon phase begins to form and where it reaches maximum size, respectively. These points are therefore revealed as changes in the slope of the spectral parameter, which is a function of the size of the fluid hydrocarbon phase. The temperatures which identify lower and upper boundaries of a lipid phase transition have been designated the lower and upper characteristic temperatures (t_l and t_h).

E. coli membranes typically display a single t_l and t_h and in this respect have properties similar to those of a binary lipid system (1–3). The phase behavior of animal cell membranes is more complex, as can be seen in Fig. 2. Spin labeled endoplasmic reticulum membranes from mouse LM cells exhibit five characteristic temperatures (Fig. 2) consistent within 1–2°C with those exhibited by LM plasma membranes and chick plasma membranes (i.e., Newcastle disease virus propagated in chick eggs) (10). The detection of

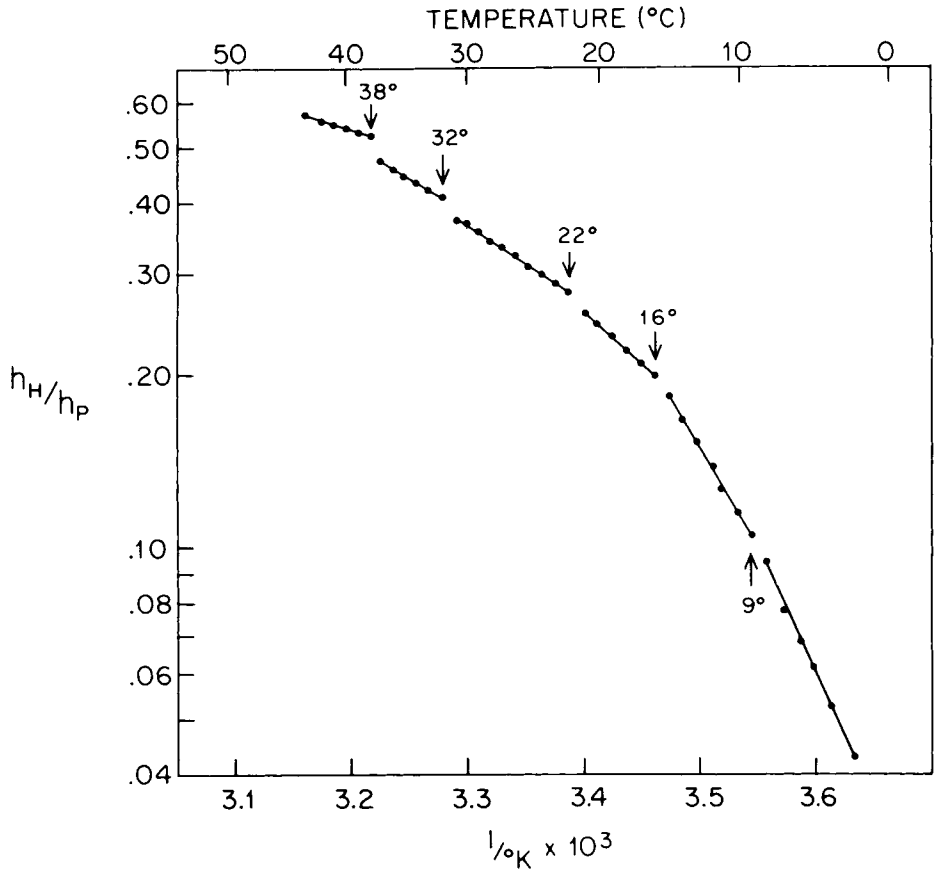

Fig. 2. Characteristic temperatures for the partitioning of the spin label 5N10 between the hydrocarbon phase of LM endoplasmic reticulum membranes and the surrounding aqueous environment. A decrease in the value of h_H/h_P indicates a loss of spin label from the hydrocarbon phase.

multiple characteristic temperatures in animal cell membranes suggests the presence of multiple lipid compartments, each displaying different phase behavior based on the physical properties of the constituent lipids.

The presence of two compartments could account for three or four of the observed characteristic temperatures depending on whether the two independent phase transitions had one or no phase boundary temperature in common. It is reasonable that the compartments could arise from an asymmetrical distribution of lipids across the bilayer of the membrane (vertical asymmetry) as well as from patching within the lateral plane of the membrane (horizontal asymmetry). A precedent for vertical asymmetry is found in the compositional asymmetry of human erythrocyte ghosts (16, 17). In these membranes, the choline-containing phosphatides are in the outer monolayer and the amino phosphatides in the inner monolayer. Our spin label data provide a means to test for the existence of two hydrocarbon compartments of approximately equal size. This is the condition that must arise from vertical asymmetry which gives rise to two physically distinct monolayers.

There are over 40 possible ways of assigning phase boundaries to two compartments from the five observed characteristic temperatures. Using the ESR spectral data shown in Fig. 3, we scrutinized the various alternatives to determine which ones were compatible with the following assumptions: (1) membrane lipid asymmetry is vertical in so far as each monolayer of the membrane bilayer exists as an independent physical entity, (2) both monolayers of the bilayer contain approximately equal amounts of lipid, (3) neither monolayer preferentially excludes or sequesters the spin label 5N10, and (4) 16°, 22°, and 32°C are valid phase boundary temperatures and cannot be omitted, reducing the number of models considered to eight. We chose to restrict our treatment to models which included these three characteristic temperatures for the following reasons. The characteristic temperatures of the cell surface membrane and the endoplasmic reticulum of LM cells are nearly identical (10), and a lateral diffusion process in the cell surface membranes of mouse fibroblasts was shown to be modified at these three temperatures (18). It is almost certain that characteristic temperatures for lateral diffusion processes are boundary temperatures for lipid phase transitions.

Implicit in assumptions (2) and (3) is the prediction that the 5N10 compartment sizes of two monolayers of the same membrane will be equal. To calculate the net amount of 5N10 incorporated into each compartment between the respective phase boundaries (i.e., Δh_H^* values), we had to ascertain whether the amount of 5N10 incorporated during the early part of the lateral phase separation process was similar to that incorporated during the later part. An examination of Model 1 (see Appendix) shows that we need to use the upper (a) and lower (b) mutually exclusive portions of the two compartments to determine the total size of the individual compartments, a+c and b+c′, respectively. When $h_H/°C$ values were calculated for each half of the phase transition, t_l to t_h, of extracted endoplasmic reticulum lipid (treatment not shown), the value for the upper half of this interval was usually about 1.25 times that of the lower half, indicating a reasonably constant uptake of spin label from the beginning to the end of the lateral phase separation process. The Appendix contains the calculations for the compartment sizes between pairs of phase boundaries specified by each model. The only models which satisfy the equality hypothesis are Models 1 and 8 (see Table I). The other six models define monolayers or compartments of grossly disproportionate sizes.

An alternative criterion by which each model was tested is best illustrated in Fig. 3 for Model 1. Briefly, the sum of the amounts of 5N10 taken up into membrane per °C in mutually exclusive portions of the two phase transitions, $h_H/°C$ (a) and $h_H/°C$ (b), should equal the $h_H/°C$ value in the region where the two phase transitions overlap (region c). Similar equations can be formulated for most of the other models (Appendix). Of the six models subject to this type of analysis, Model 1 is the only model which satisfies the specified criterion. Model 8, unfortunately, is not amenable to this type of analysis. We favor Model 1 since this very same model best fits the data for two lipid compartments of equal size for the membrane envelope of the paramyxovirus, Newcastle disease virus (i.e., a membrane equivalent to the plasma membrane of the chick cell host) (10).

When lipids were extracted from the endoplasmic reticulum of LM cells for spin label studies, only two characteristic temperatures were revealed, 16° and 35°C (Fig. 4). The results of this experiment indicate that the characteristic temperatures of the membrane lipids in situ arise from their organization within the membrane. The t_h value of the extracted lipid is approximately midway between the t_h and t_h' values specified by

TABLE I. Assessment of Possible Boundaries† for Lateral Phase Separations of Lipids in Endoplasmic Reticulum Membranes of LM Cells

Model	Phase boundaries t_l' to t_h' = °C* t_l to t_h = °C*	Interval (°C) for calculation of h_H/°C	$\frac{h_H‡}{°C}$	Δh_H*††
1	(22 to 38) = 16	(32 to 38)	0.18/6 = 0.0300	0.480
	(16 to 32) = 16	(16 to 22)	0.23/6 = 0.0383	0.613
8	(32 to 38) = 6	(32 to 38)	0.18/6 = 0.0300	0.180
	(16 to 22) = 6	(16 to 22)	0.23/6 = 0.0383	0.230

†Eight of more than 40 possible models were considered. Evidence from cell surface antigen mixing experiments indicates characteristic temperatures in the rate of lateral mobility of cell surface antigens occurring at approximately 16°, 22°, and 32°C (18). These temperatures are almost certain to be phase boundaries. Since both the cell surface membrane and endoplasmic reticulum fractions have nearly identical characteristic temperatures, we chose to consider only those models that include these three temperatures as possible phase boundaries. The assumptions and calculations for the eight models are presented in the Appendix.

‡The measured values of h_H at the five possible critical temperatures exhibited by spin labeled LM endoplasmic reticulum (see Materials and Methods; Fig. 3) were: 38°, 1.81 cm; 32°, 1.63 cm; 22°, 1.05 cm; 16°, 0.82 cm; and 9°, 0.60 cm. The parameter h_H/°C expresses the net change in h_H per °C.

††$\frac{h_H}{°C} \times$ °C* = Δh_H* which represents the net change in h_H between the phase boundaries of the model.

Model 1 (32° and 38°C). The t_l value for the extracted lipid was close to the lower of the two t_l values specified by this model. It should be noted, however, that the t_l value of lipids extracted from E. coli membranes were approximately 4.5–7° lower than the t_l values obtained with the membranes from which they were extracted (3). Thus, the t_l value observed for the extracted lipids could be an "average" of the two t_l values for the independent monolayers depicted in Model 1.

DISCUSSION

ESR analysis of the endoplasmic reticulum fraction from a cultured mouse fibroblast line (LM cells) reveals that the lipids are in a more complex organization in the membrane than they are following extraction and dispersal in aqueous medium. Five characteristic temperatures were detected with the membrane fraction (Fig. 2), but only two were observed with the aqueous dispersion of lipids extracted from these membranes (Fig. 4). Companion ESR studies with LM cell surface membranes and Newcastle disease virus (NDV), a membrane-enveloped paramyxovirus which was propagated in chick eggs, revealed five and four characteristic temperatures, respectively (10), and all these were within 1–2° of the corresponding characteristic temperatures reported here for LM cell endoplasmic reticulum membranes (Table II). Aside from showing that membranes from these animal sources are more complex than those of bacteria where only two characteristic temperatures are normally detected, these studies indicate that membranes from different homeothermic vertebrates (mouse and chick) have similar physical properties.

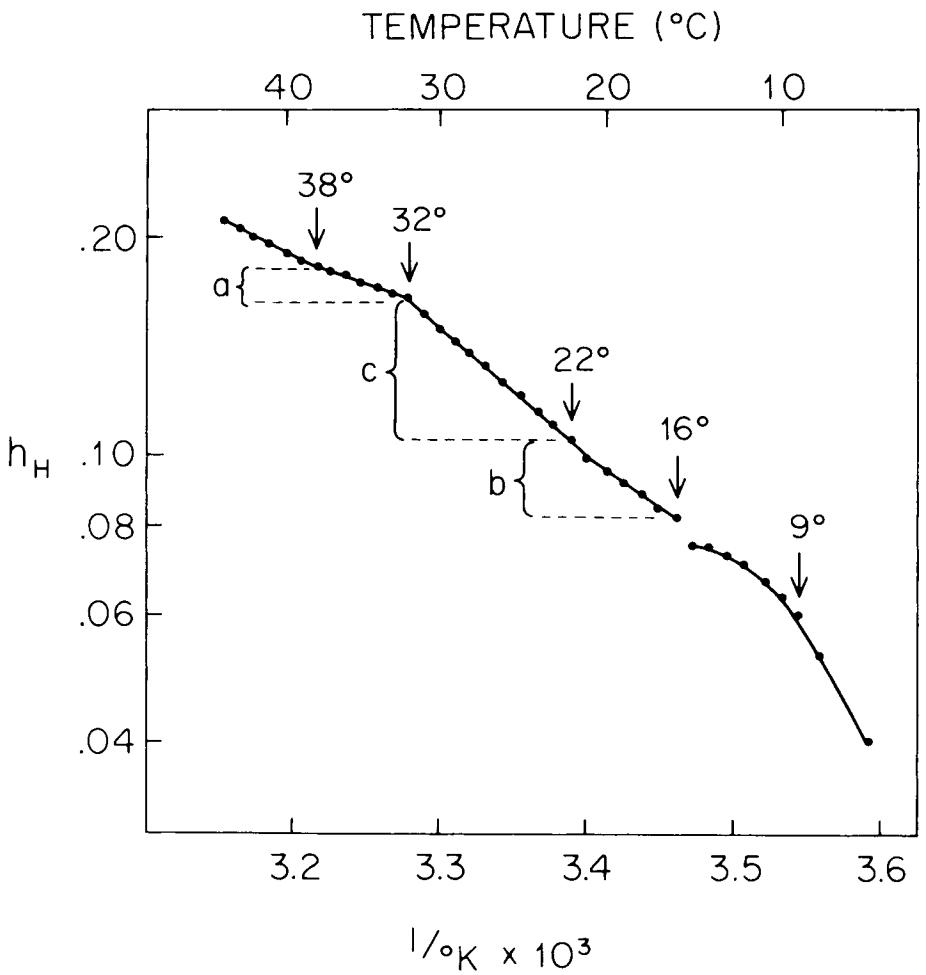

Fig. 3. Arrhenius plot showing the increase in the hydrocarbon component (h_H in decimeters) of the ESR signal from spin labeled LM endoplasmic reticulum with increasing temperature. Regions a and b define mutually exclusive intervals of lateral phase separations – that is, areas restricted to one or the other monolayer of hypothetical Model 1 (Table I). Region c defines the interval where both monolayers are simultaneously undergoing lateral phase separations.

The ESR data were analyzed to test the possibility that the two monolayers of the endoplasmic reticulum bilayer have different phase transitions. This analysis was predicated on the reasoning that these two lipid compartments should be of approximately equal size, and two models (Models 1 and 8) were found to satisfy this condition within a reasonable limit of error. Of these, Model 1 best satisfied this condition. This same model also came closest to satisfying this condition in a treatment of ESR data obtained with NDV (Table II and ref. 10). In the case of the cell surface membrane, there was sufficient physiological information to further decide between the models that satisfied the equality condition and to permit a tentative assignment of a given set of phase boundaries to a given monolayer. In these studies we concluded that our data were

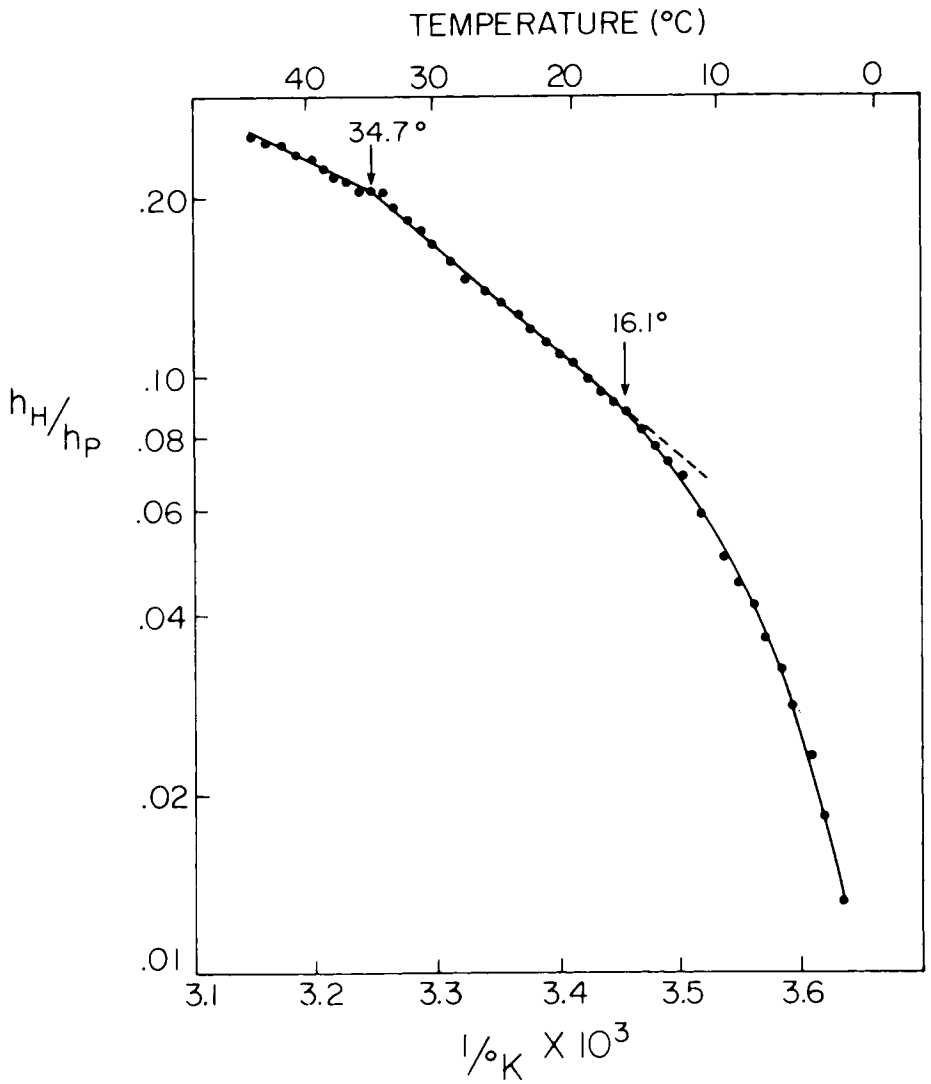

Fig. 4. Characteristic temperatures for partitioning of the spin label 5N10 between the hydrocarbon phase of lipids extracted from LM endoplasmic reticulum membranes and the surrounding aqueous environment (see Materials and Methods for details).

most compatible with a model for the cell surface membrane in which the phase boundaries of the inner and outer monolayers were approximately 21° and 37°C, and 15° and 31°C, respectively. The physiological data which permitted these assignments are shown in Table II, and more extensive treatments have been published (5, 10). One of the most important pieces of physiological information is that of Keirns et al. (23), namely that the hormone (glucagon or epinephrine) stimulated adenyl cyclase activities of rat liver have a characteristic temperature of approximately 30°C, but basal adenyl cyclase activity does not. Since hormone receptors reside on the external cell surface, a

TABLE II. Physical and Physiological Characteristic Temperatures of Animal Cell Membranes

5N10 Partitioning	Characteristic temperatures (°C)[a]			
	$t_{l(o)}$	$t_{l(i)}$	$t_{h(o)}$	$t_{h(i)}$
LM endoplasmic reticulum	16	22	32	38
LM plasma membrane (10)	15	21	30	37
Egg-grown NDV_{HP} (10)	14	22	32	38
Physiological parameters	$^*t_{l(o)}$	$^*t_{l(i)}$	$^*t_{h(o)}$	$^*t_{h(i)}$
α-Aminoisobutyrate transport (LM cells; 10)	16	20	29	37
$Na^+ + K^+ + Mg^{++}$-ATPase (LM cell plasma membrane; 10)	15	23	28–31	37
Con A binding by LM cells (19, 20)	15–19			
Con A binding by Py3T3 cells (21)	15			
Con A-mediated hemadsorption by LM cells (19, 20)	13–15			
Con A-mediated agglutination with Py3T3 cells (22)	15			
Basal adenyl cyclase of rat liver[b]		22	–	36–38
Hormone-stimulated adenyl cyclase of rat liver (23)[b]		22	32	?
Rate of mixing of mouse and human cell surface antigens after cell fusion (18)	15[c]	21	28–30	
Cessation of growth of LM cells[d]		23		

[a]The symbols $t_{l(o)}$, $t_{l(i)}$, $t_{h(o)}$, and $t_{h(i)}$ refer to the cell surface membrane only and are the lower characteristic temperatures of the outer and inner monolayers and the upper characteristic temperatures of the outer and inner monolayers, respectively. The assignment of two sets of characteristic temperatures is based on the calculations given in Table I, and the assignments of these sets to the inner and outer monolayers are based on the physiological parameters presented in this table. The rationale for these assignments is presented elsewhere (5, 10).

[b]The characteristic temperature for basal adenyl cyclase at approximately 22°C was observed by J. Keirns (personal communication). The characteristic temperature at approximately 36–38°C can be detected in Fig. 1 of the data published by Keirns et al. (23). The published data do not preclude a characteristic temperature for hormone-stimulated activity at 36–38°C, and the lowest temperature for activity analysis was 20°C in the published experiments.

[c]The rate of antigen mixing, a measure of protein mobility on the cell surface, decreased slowly from 42° to 30°C. Below 30°C, the rate of antigen mixing declined rapidly to a minimum at 21°C and then increased from 21° to 15°C. A precipitous drop in the rate of mixing occurred below 15°C.

[d]Cells for the inoculum were grown at 37°C in MEM + P medium (Materials and Methods), and tests for growth at various temperatures were also in MEM + P (Rittenhouse, H. G., and Williams, R. E., unpublished observations).

characteristic temperature of about 30°C is likely to be a property of the outer monolayer.

There is a real paucity of physiological thermotropic data for endoplasmic reticulum compared with the current status of availability of information on the cell surface membrane. Eletr et al. (24) have examined the response of UDP-glucuronyl transferase and glucose-6-phosphatase activity in guinea pig liver microsomes over the temperature range 6–40°C and reported characteristic temperatures of 19° and 32°C, and 19°C, respectively. Their assays, however, were at intervals of 3–4°C, and it has been our experience that

assays at 1° intervals are required for the detection of all the characteristic temperatures for membrane-associated activities. Recently, Lynn Grinna and Albert Barber at the University of California, Los Angeles (unpublished observations) have studied the response to temperature of glucose-6-phosphatase in microsomes from both rat liver and kidney. They have detected four characteristic temperatures which correlate with the characteristic temperatures reported here for endoplasmic reticulum from cultured mouse cells.

Though our data certainly point to physical asymmetry in the surface membrane and endoplasmic reticulum, the physiological significance of this asymmetry is not known. This physical asymmetry could arise from sidedness in the distribution of polar headgroups in membrane phospholipids as reported by Bretscher (16) and by van Deenen and his associates (17). As shown by Träuble and his coworkers, polar headgroup composition and other ionic factors can influence the characteristic temperatures for the melting of phospholipids (25). It will be interesting to see if the endoplasmic reticulum is also characterized by polar headgroup sidedness. The assignment of a particular set of boundary temperatures to a particular endoplasmic reticulum monolayer (intracysternal vs extracysternal) should also allow an interesting test of hypotheses which stipulate that the cell surface membrane is generated from endoplasmic reticulum vesicles by a fusion process.

ACKNOWLEDGMENTS

This work was supported by research grant GM-18233 from the United States Public Health Service. C. Fred Fox is the recipient of a Research Career Development Award from USPHS, and Bernadine J. Wisnieski is a Celeste Durand Rogers Fellow in Cancer Research. We are grateful to Dr. Alec Keith of Pennsylvania State University for providing us with the spin label employed in these studies.

REFERENCES

1. Linden, C. D., and Fox, C. F., J. Supramol. Struc. 1:535 (1973).
2. Linden, C. D., Keith, A. D., and Fox, C. F., J. Supramol. Struc. 1:523 (1973).
3. Linden, C. D., Wright, K. L., McConnell, H. M., and Fox, C. F., Proc. Nat. Acad. Sci. U.S. 70:2271 (1973).
4. Machtiger, N. A., and Fox, C. F., Ann. Rev. Biochem. 42:575 (1973).
5. Fox, C. F., in "Cell Walls and Membranes, MTP Reviews of Science: Biochemistry," C. F. Fox (Ed.). (Butterworths, London (in press).
6. Tsukagoshi, N., and Fox, C. F., Biochemistry 12:2822 (1973).
7. Tsukagoshi, N., and Fox, C. F., Biochemistry 12:2816 (1973).
8. Overath, P., Schairer, H. U., and Stoffel, W., Proc. Nat. Acad. Sci. U.S. 67:606 (1970).
9. McElhaney, R. N., J. Supra. Struc. 2:618 (1974).
10. Wisnieski, B. J., Parkes, J. G., Huang, Y. O., and Fox, C. F., Proc. Nat. Acad. Sci. U.S. 71:4381 (1974).
11. Wisnieski, B. J., Williams, R. E., and Fox, C. F., Proc. Nat. Acad. Sci. U.S. 70:3669 (1973).
12. Schimmel, S. D., Kent, C., Bischoff, R., and Vagelos, P. R., Proc. Nat. Acad. Sci. U.S. 70:3195 (1973).
13. Bligh, E. G., and Dyer, W. J., Can. J. Biochem. Physiol. 37:911 (1959).
14. Shimshick, E. J., and McConnell, H. M., Biochemistry 12:2351 (1973).

15. Hubbell, W. L., and McConnell, H. M., Proc. Nat. Acad. Sci. U.S. 61:12 (1968).
16. Bretscher, M. S., Nature New Biol. 236:11 (1972).
17. Verkleij, A. J., Zwaal, R. F. A., Roelofsen, B., Comfurius, P., Kastelijn, D., and van Deenen, L. L. M., Biochim. Biophys. Acta 323:178 (1973).
18. Petit, V. A., and Edidin, M., Science 184:1183 (1974).
19. Rittenhouse, H. G., and Fox, C. F., Biochem. Biophys. Res. Commun. 57:323 (1974).
20. Rittenhouse, H. G., Williams, R. E., Wisnieski, B., and Fox, C. F., Biochem. Biophys. Res. Commun. 58:222 (1974).
21. Noonan, K. D., and Burger, M. M., J. Biol. Chem. 248:4286 (1973).
22. Noonan, K. D., and Burger, M. M., J. Cell Biol. 59:134 (1973).
23. Keirns, J. J., Kreiner, P. W., and Bitensky, M. W., J. Supramol. Struc. 1:368 (1973).
24. Eletr, S., Zakim, D., and Vessey, D. A., J. Mol. Biol. 78:351 (1973).
25. Träuble, H., and Eibl, H., Proc. Nat. Acad. Sci. U.S. 71:214 (1974).

APPENDIX

Calculation of sizes of 5N10 hydrocarbon partitioning compartments for membrane models in which the bilayer is assumed to consist of two monolayer compartments of approximately equal size.†

Model 1

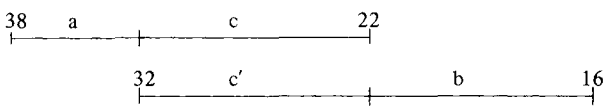

‡**Condition I:**	h_H/°C (a) +	h_H/°C (b) =	h_H/°C (c + c′)
does	0.18/6	+0.23/6	=0.58/10
does	0.0300	+0.0383	=0.0580
	0.0683		≅0.0580

††**Condition II:**	h_H/°C (a) × °C (a + c)	=h_H/°C (b) × °C (b + c′)	
	or Δh_H* (a + c)	=Δh_H* (b + c′)	
does	0.18/6 × 16	=0.23/6 × 16	
does	0.0300 × 16	=0.0383 × 16	
	0.480	≅0.613	

Model 2

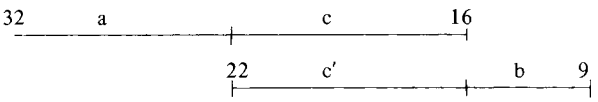

Condition I:	h_H/°C (a) +	h_H/°C (b)	$=h_H$/°C (c + c')
does	0.58/10	+0.22/7	=0.23/6
does	0.0580	+0.0314	=0.0383
	0.0894		≠0.0383
Condition II:	h_H/°C (a) × °C (a + c)		$=h_H$/°C (b) × °C (b + c')
	or Δh_H* (a + c)		$=\Delta h_H$* (b + c')
does	0.58/10 × 16		=0.22/7 × 13
does	0.0580 × 16		=0.0314 × 13
	0.928		≠0.409

Model 3

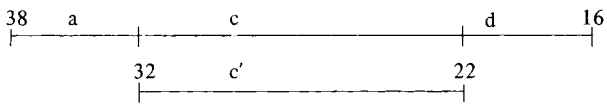

Condition I:	h_H/°C (a)	$=h_H$/°C (d)
does	0.18/6	=0.23/6
	0.0300	≅0.0383
Condition II:	h_H/°C (a) × °C (a+c+d)	$=h_H$/°C (c+c') × °C (c) − h_H/°C (a) × °C (c)
	or Δh_H* (a+c+d)	$=\Delta h_H$* (c') where °C (c) = °C (c')
does	0.18/6 × 22	=0.58/10 × 10 − 0.18/6 × 10
does	0.0300 × 22	=0.0580 × 10 − 0.0300 × 10
does	0.66	=0.58 − 0.30
	0.66	≠0.28
Condition II (Alternate):	h_H/°C (d) × °C (a+c+d)	$=h_H$/°C (c+c') × °C (c) − h_H/°C (d) × °C (c)
	or Δh_H*(a + c + d)	= Δh_H* (c')
does	0.23/6 × 22	=0.58/10 × 10 − 0.23/6 × 10
does	0.0383 × 22	=0.0580 × 10 − 0.0383 × 10
does	0.843	=0.580 − 0.383
	0.843	≠0.197

Model 4

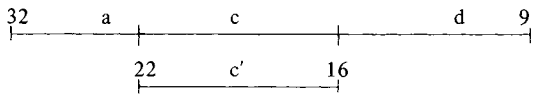

Condition I:	h_H/°C (a)	= h_H/°C (d)
does	0.58/10	=0.22/7
	0.0580	≠0.0314
Condition II:	h_H/°C (a) × °C (a + c + d)	=h_H/°C(c+c') × °C (c) – h_H/°C (a) × °C (c)
	or Δh_H* (a + c + d)	=Δh_H* (c') where °C (c) = °C (c')
does	0.58/10 × 23	=0.23/6 × 6 – 0.58/10 × 6
does	0.0580 × 23	=0.0383 × 6 – 0.0580 × 6
does	1.334	=0.230 – 0.348
	1.334	≠ –0.118
Condition II	h_H/°C (d) × °C (a + c + d)	=h_H/°C (c+c') × °C (c) – h_H/°C (d) × °C (c)
(Alternate):	or Δh_H* (a + c + d)	=Δh_H* (c')
does	0.22/7 × 23	=0.23/6 × 6 – 0.22/7 × 6
does	0.0314 × 23	=0.0383 × 6 – 0.0314 × 6
does	0.722	=0.230 – 0.188
	0.722	≠0.042

Model 5

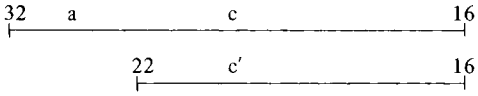

Condition I:	h_H/°C (c + c')	>2 × h_H/°C (a)
does	0.23/6	>2 × 0.58/10
does	0.0383	>2 × 0.0580
	0.0383	≯0.116
Condition II:	h_H/°C (a) × °C (a + c)	=h_H/°C (c+c') × °C (c) – h_H/°C (a) × °C (c)
	or Δh_H* (a + c)	=Δh_H* (c') where °C (c) = °C (c')
does	0.58/10 × 16	=0.23/6 × 6 – 0.58/10 × 6
does	0.0580 × 16	=0.0383 × 6 – 0.0580 × 6
does	0.928	=0.230 – 0.348
	0.928	≠ –0.118

Model 6

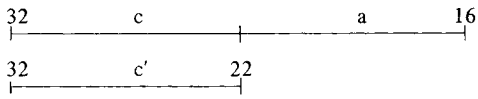

Condition I:	h_H/°C (c + c')	>2 × h_H/°C (a)
does	0.58/10	>2 × 0.23/6
does	0.0580	>2 × 0.0383
	0.0580	≯0.0766
Condition II:	h_H/°C (a) × °C (a + c)	=h_H/°C (c+c') × °C (c) − h_H/°C (a) × °C (c)
	or Δh_H* (a + c)	=Δh_H* (c') where °C (c) = °C (c')
does	0.23/6 × 16	=0.58/10 × 6 − 0.23/6 × 6
does	0.0383 × 16	=0.0580 × 6 − 0.0383 × 6
does	0.613	=0.348 − 0.230
	0.613	≠0.118

Model 7

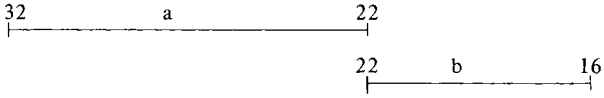

Condition I:	h_H/°C (a) may or may not equal h_H/°C (b)	
	0.58/10	≠0.23/6
	0.0580	≠0.0383
Condition II:	h_H/°C (a) × °C (a)	≈h_H/°C (b) × °C (b)
	Δh_H* (a)	≈Δh_H* (b)
does	0.58/10 × 10	=0.23/6 × 6
does	0.0580 × 10	=0.0383 × 6
	0.580	≠0.230

Model 8

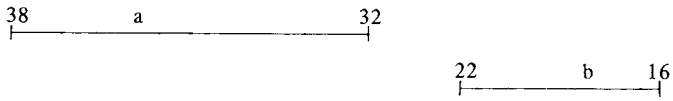

Condition I:	h_H/°C (a) may or may not equal h_H/°C (b)	
	0.18/6	=0.23/6
	0.0300	≅0.0383
Condition II:	h_H/°C (a) × °C (a)	=h_H/°C (b) × °C (b)
	Δh_H* (a)	=Δh_H* (b)
does	0.18/6 × 6	=0.23/6 × 6
does	0.0300 × 6	=0.0383 × 6
	0.180	≅0.230

†This assessment of possible phase boundaries further assumes that neither monolayer preferentially sequesters or excludes spin label.

‡h_H/°C is an empirical estimate of the amount of 5N10 uptake per °C by a membranous compartment.

††Δh_H* is an empirical estimate of the net incorporation of 5N10 by a membranous compartment over a defined interval.